Article

# Effects of Antibody Binding on Structural Transitions of the Nicotinic Acetylcholine Receptor

Shiori Tamamizu, Daniel H. Butler, Jos A. Lasalde, and Mark G. McNamee

*Biochemistry*, **1996**, 35 (36), 11773-11781 • DOI: 10.1021/bi960369u

# Effects of Antibody Binding on Structural Transitions of the Nicotinic Acetylcholine Receptor†

Shiori Tamamizu, Daniel H. Butler, José A. Lasalde, and Mark G. McNamee*

*Section of Molecular and Cellular Biology, University of California, Davis, California 95616*

*Received February 16, 1996; Revised Manuscript Received July 12, 1996*⊗

ABSTRACT: Patch-clamping and photoaffinity-labeling techniques were used to study the effects of binding of monoclonal antibodies (mAbs) on the function of *Torpedo californica* nicotinic acetylcholine receptor (nAChR). The rat anti-*Torpedo* nAChR mAbs examined here are known to inhibit ligand binding to either the high-affinity (mAb 247) or both the high- and low−affinity binding sites (mAb 370 and mAb 387) [Mihovilovic, M. & Richman, D. P. (1984) *J. Biol. Chem. 259*, 15051−15059; Mihovilovic, M., & Richman, D. P. (1987) *J. Biol. Chem. 262*, 4978−4986]. Single-channel analysis shows that mAb 247 and the Fab fragment of mAb 247 inhibit the opening of the nAChR ion channel, although they have no effects on the structural transition from the resting to desensitized state as monitored by the extent of decreased labeling by the photoreactive probe 3-(trifluoromethyl)-3-(*m*-[$^{125}$I]iodophenyl)diazirine ([$^{125}$I]-TID). In the presence of mAb 387, the nAChR single-channel amplitude was decreased by 20%, whereas Fab 387 completely inhibited channel opening. [$^{125}$I-TID]-labeling studies suggest that the mAb 387−nAChR and Fab 387−nAChR complexes are able to undergo the transition between resting and desensitized states. This result confirms that the nAChR can assume a desensitized state without prior channel opening. In addition, mAb 35 and mAb 132, which recognize the main immunogenic region (MIR) of the nAChR, and mAb 370 do not alter either single-channel behavior or labeling patterns. Combining the results from characterization with respect to their epitopes and their effects on agonist (carbamylcholine) and antagonist [α-bungarotoxin (α-BTX) and curare] binding, these results indicate that mAbs could be used to map functional and structural domains.

Nicotinic acetylcholine receptors (nAChR)[1] are members of a family of ligand-gated ion channels, which includes glycine, $GABA_A$, and $5\text{-}HT_3$ receptors (Betz, 1990; Unwin, 1993). The pentameric nAChR from the electric organ of *Torpedo californica* consists of four types of homologous subunits with a stoichiometry of $\alpha{:}2\beta{:}\gamma{:}\delta$ [for reviews, see Conti-Tronconi et al. (1994), Karlin (1993), and Pradier and McNamee (1992)]. Each subunit contains four hydrophobic domains designated as M1, M2, M3, and M4, which are proposed as transmembrane crossings (Mishina et al., 1984; Noda et al., 1983). The N terminal makes up the large extracellular domain which contains the agonist binding site (DiPaola et al., 1989). Upon the binding of acetylcholine, the receptor opens a cation channel which depolarizes the postsynaptic membrane. Prolonged incubation of nAChR with high concentrations of activating ligands induces the receptor to undergo a transition into a desensitized state (Ochoa et al., 1989). In the desensitized state, the ion channel is no longer open, although it has an increased affinity for acetylcholine binding.

Table 1: Characteristics of Binding of mAb to nAChR from Competition ELISA and Peptide-Mapping Studies[a]

| mAb | carb | α-BTX | curare | location |
|---|---|---|---|---|
| 35 | − | − | − | α67−76 |
| 132 | − | − | − | α67−76 |
| 247 | − | ↓(50%) | ↓ | ? |
| 370 | ↓ | ↓ | ↓ | α187−205 |
| 371 | − | − | − | α67−76? |
| 383 | ↓ | ↓ | ↑ | α187−199 |
| 387 | ↓ | ↓ | ↑ | ? |

[a] Data and mAbs were provided by Drs. David Richman, Robert Fairclough, and Jon Lindstorm (Gomez et al., 1983; Donnelly et al., 1984; Mihovilovic et al., 1984, 1987; Chinchetru et al., 1989; Fairclough et al., 1993; Xu et al., 1993a,b). ↓ and ↑, effect on binding; −, no effect on binding.

Binding studies of monoclonal antibodies (mAbs) or polyclonal antibodies raised against a specifc region of protein have been used as tools to study the relationships of structure and function of ion channels (Beck et al., 1994; Valenzuela et al., 1994). By identification of the epitope as well as the functional consequences of antibody binding, it is possible to assign specific channel operations to linear or conformationally defined regions of the nAChR. The rat anti-*Torpedo* nAChR mAbs used in this study have been characterized with respect to their epitopes and their effects on agonist and antagonist binding as summarized in Table 1. mAb 370 and mAb 387 inhibit binding of the agonist carbamylcholine (carb) and differentiate between subsites within the cholinergic site (Watters & Maelicke, 1983; Mihovilovic et al., 1984, 1987). mAb 247 can block only 50% of α-bungarotoxin (α-BTX) binding without altering the affinity of agonist for the nAChR, indicating that mAb

† This research was supported by a research grant to M.G.M. from the National Institutes of Health (NS22941).

* Corresponding author: Dr. Mark McNamee, Section of Molecular and Cellular Biology, University of California, Davis, CA 95616. Phone: (916) 752−6764. Fax: (916) 752-2604. E-mail: mgmcnamee@ucdavis.edu.

⊗ Abstract published in *Advance ACS Abstracts,* August 15, 1996.

[1] Abbreviations: mAb, monoclonal antibody; nAChR, nicotinic acetylcholine receptor; TID, 3-(trifluoromethyl)-3-(*m*-iodophenyl)-diazirine; MIR, main immunogenic region; carb, carbamylcholine; α-BTX, α-bungarotoxin; d-Tc, *d*-tubocurare; ELISA, enzyme-linked immunosorbent assay; PC, phosphatidylcholine; PA, phosphatidic acid; CH, cholesterol.

S0006-2960(96)00369-8 CCC: $12.00 

247 can differentiate between the two nAChR α-BTX binding sites (Mihovilovic et al., 1984; Dowding & Hall, 1987).

Here, we report the functional studies of mAb−nAChR interactions. The effects of the antibodies were examined by patch clamp methods on *T. californica* nAChR expressed in *Xenopus laevis* oocytes. Patch clamp allows the observation of the single-channel behavior of mAb−nAChR and Fab−nAChR complexes. In addition to wild type, we used a mutant nAChR which has an increased channel open time (Lasalde et al., 1995). The longer open time of the mutant allows easier detection of any changes in open time caused by the binding of mAbs. In parallel, mAbs were used in photolabeling experiments with nAChR purified from *Torpedo* electroplax tissue. This technique was used to monitor the resting to desensitized transitions of the antibody−nAChR complexes. 3-(Trifluoromethyl)-3-(*m*-[$^{125}$I]iodophenyl)diazirine ([$^{125}$I]TID) photolabels each of the subunits when the nAChR is in the resting state. In the presence of high concentrations of the agonist, the level of [$^{125}$I]TID labeling decreases significantly (McCarthy & Stroud, 1989; White et al., 1991, Blanton & Cohen, 1992, 1994; White & Cohen, 1992). The agonist-sensitive photolabeling sites have been mapped to the M2 region of nAChR (White & Cohen, 1992). It is presumed that the incorporation efficiency of [$^{125}$I]TID is reduced due to the conformational change accompanying receptor desensitization (White & Cohen, 1992). In this study, we find that mAb 247 and mAb 387 can alter the single-channel behavior of nAChR without affecting the transition from the resting to the desensitized state, whereas binding of mAb 370 does not affect the functional behavior of nAChR. The results are discussed in terms of how these antibodies provide new information about nAChR structure and function.

## MATERIALS AND METHODS

*Materials.* DEAE-cellulose, goat anti-rat horseradish peroxidase, *o*-phenylenediamine dihydrochloride (OPD), and cholesterol hemisuccinate (CH) were obtained from Sigma (St. Louis, MO). Synthetic dioleoylphosphatidylcholine (PC) and dioleoylphosphatidic acid (PA) were obtained from Avanti Polar Lipids (Birmingham, AL). 3-(Trifluoromethyl) 3-*m*-[$^{125}$I]iodophenyl)diazirine ([$^{125}$I]TID) was purchased from Amersham (Arlington Heights, IL).

*Monoclonal Antibody Purification.* The supernatants containing anti-*Torpedo* nAChR mAbs from hybridoma cultures (fused spleen cells from a rat immunized with *Torpedo* nAChR with a mouse myeloma cell line) were generous gifts from Dr. David Richman and Dr. Robert Fairclough, University of California, Davis, CA (Gomez & Richman, 1985). All procedures were carried out at 4 °C. Approximately 500 mL of hybridoma supernatant was concentrated to 50 mL in a stirred-cell apparatus (Amicon, Beverly, MA) containing a YM-100 membrane. The solution was dialyzed overnight against 4 L of 10 mM sodium phosphate (pH 7.8) (buffer A) and applied to a 3 ×10 cm DEAE-cellulose column equilibrated in buffer A. The flow-through fractions with an $A_{280}$ greater than 0.1 absorbance unit were pooled and concentrated in an Amicon Centriprep-100 device centrifuged at 1000*g* for 50 min.

*Production of Fab Fragments.* Fab fragments were generated from purified mAb stocks by digestion with immobilized papain (Pierce, Rockford, IL). The digestion procedure is described in instructions provided by Pierce. Briefly, 1−4 mg of mAb in 0.5 mL was dialyzed overnight against 20 mM sodium phosphate and 10 mM EDTA (pH 7.0) (molecular weight cutoff of 12−14K). The mAb solution was added to 0.5 mL of digestion buffer [20 mM sodium phosphate, 10 mM EDTA, and 20 mM cysteine hydrochloride (pH 7.0)] and 0.5 mL of the immobilized papain slurry previously equilibrated in the digestion buffer. The tube was incubated at 37 °C and shaken at 60 rpm for 24 h. The tube was briefly centrifuged, and the supernatant was removed and concentrated in an Amicon Centricon-10 concentrator.

*Characterization of mAbs and Fab Fragments.* The purity of mAbs and Fabs was ascertained by 12% SDS−polyacrylamide gel electrophoresis (SDS−PAGE) under reducing and nonreducing conditions followed by Commassie blue staining. The protein concentration was measured by the Lowry method (Lowry et al., 1951).

Fab and mAb binding was determined by an enzyme-linked immunosorbent assay (ELISA) (Mihovilovic et al., 1987). Plates were coated overnight with 0.1 mL of 10 nM purified *T. californica* nAChR (see below). After removal of the nAChR solution, 0.2 mL of 1% BSA in phosphate-buffered saline (PBS) was added for 2 h to block nonspecific sites. The BSA/PBS solution was removed, and 0.1 mL of 50 mg/mL mAb or Fab was added. The plate was washed six times with PBS buffer after the 1 h antibody incubation. Goat anti-rat horseradish peroxidase (100 $\mu$L) was added and the mixture incubated for 1 h at room temperature. The plate was washed six times, and substrate buffer was added [0.1 M citrate (pH 4.7), 0.83 mg/mL OPD, and 0.1% hydrogen peroxide]. The plate was allowed to develop for 30 min in the dark, and the absorbances were recorded by a plate reader at 450 nm.

*Oocyte Expression System.* cDNAs of *T. californica* nAChR subunits in pSP64 plasmid were linearized by *Sma*I and transcribed *in vitro* with Megascript SP6 (Ambion, Austin, TX). Mixtures of cRNAs were prepared with the stoichiometry 2:4:1:1 ($\alpha$:$\beta$:$\gamma$:$\delta$). (Since the level of $\beta$ subunit was found to limit overall receptor expression, the amount of $\beta$ subunit RNA was increased up to 4 times relative to those of $\gamma$ and $\delta$ subunits.) Defolliculated *X. laevis* oocytes were obtained as described previously (Li et al., 1990). Fifty nanoloiters of the RNA mixture at the concentration of 0.4 $\mu$g/$\mu$L was injected into each oocyte with a digital microdispenser. Oocytes were transferred into petri dishes containing Leibovitz's L-15 medium and stored in a 18−19 °C incubator.

*Single-Channel Analysis of mAb−nAChR Interactions.* The oocyte vitelline envelope was removed manually after incubation in hyperosmotic solution [150 mM NaCl, 2 mM KCl, 3% sucrose, and 5 mM HEPES (pH 7.6)]. The oocytes were placed into a recording chamber constantly perfused with bath solution [100 mM KCl, 1 mM $MgCl_2$, and 10 mM HEPES pH 7.2)] at 18 °C. The patch pipettes were constructed of Sutter thick-walled borosilicate glass (Novato, CA) and were pulled to exhibit resistances of 8−12 MΩ. The pipette solution contained 100 mM KCl, 10 mM HEPES, 10 mM EGTA (pH 7.2), and 4$\mu$M ACh. The pipette included 10 $\mu$g/$\mu$L mAb or Fab. All experiments were performed in a cell-attached patch configuration. Patches were stable for about 1 h after seal formation, which allows

examination of channel behavior after exposure to mAbs. A Dagan 3900 (Minneapolis, MN) apparatus with a headstage resistor (10 GΩ) was used to amplify the channel currents which were filtered at 5 kHz (3 dB; 8-pole Bessel) and stored on a digital data recorder (94 kHz sampling; Instrutech VR-10 apparatus, Mineola, NY). Data were played back into an 80486-based computer through a TL-1 DMA digital interface (Axon Instruments, Foster City, CA) as an analog signal with redigitalization at 50 kHz (FETCHEX, Axon Instruments). Records were digitally filtered (Gaussian low-pass filter; net effective frequency of 4−7 kHz), and single-channel currents were detected with a half-amplitude crossing algorithm (IPROC; Sachs et al., 1982). Data analysis was performed using pCLAMP (Axon Instruments).

*Acetylcholine Receptor Purification.* nAChR was purified from *T. californica* electroplax tissue by affinity chromatography (Ochoa et al., 1983). Protein and phosphate assays were utilized to determine the lipid:protein ratios (Lowry et al., 1951; McClare, 1971). Purified nAChRs were reconstituted into phosphatidylcholine (PC)/phosphatidic acid (PA)/cholesterol (CH) membranes at a 60:20:20 molar ratio and a 1:1500 protein:lipid ratio as described previously (McNamee et al., 1986). All experiments were performed with DB-1 [100 mM NaCl, 10 mM MOPS, 0.1 mM EDTA, and 0.02% $NaN_3$ pH 7.4)] as the buffer. Receptor samples were stored at 4 °C until they were ready for use.

*[$^{125}$I]TID Photolabeling of nAChR.* All experiments were carried out at room temperature in the dark. Approximately 56 pmol of purified nAChR was incubated with 100−150 pmol of purified active mAb or Fab for 30 min. Carbamylcholine (carb) was then added to the reaction mixture to a concentration of 1 mM and incubated for 5 min. The [$^{125}$I]-TID was pipetted into the mixture to a final concentration of 1−2 $\mu$M. After a 15 min incubation, samples were irradiated for 10 min with ultraviolet light (365 nm). Thirty microliters of the reaction mixture was combined with 30 $\mu$L of electrophoresis loading buffer and 3 $\mu$L of $\beta$-mercaptoethanol. SDS−PAGE was performed on a 7.5% premade acrylamide gel (Bio-Rad, Hercules, CA). The gel was dried overnight and the subunit bands were visualized using a BAS1000 or BAS2000 phosphorimager (Fuji Medical Systems, Stamford, CT) and standard autoradiography.

*Analysis of Photolabeling Experiments.* The phosphorimager files were imported into NIH Image software (National Institutes of Health, Bethesda, MD). The average density of each nAChR $\gamma$-subunit band was measured. The density was multiplied by the area of the analysis window to obtain the raw counts per band. This value was subtracted from the background to receive the actual counts per band. The background of each lane was determined by finding the counts in analysis window placed between the $\gamma$- and $\delta$-subunit. The gel images were then imported into Photoshop (Adobe Systems) for contrast enhancement and preparation of photographs.

## RESULTS

*Patch Clamp Analysis of Antibody−nAChR Complexes.* *X. laevis* oocytes expressing wild type or a mutant *T. californica* nAChR were used to investigate the functional effects of mAbs and Fabs. As we previously reported (Lasalde et al., 1995), a point mutation from Gly to Trp at position 421 of the α-subunit (αG421W) increases channel open time without affecting $EC_{50}$ for acetylcholine (ACh). This longer open time of the αG421W mutant permits easier identification of alterations in single-channel behavior. Since the mutation is located in the M4 transmembrane domain and far from any of the extracellular epitopes, it is presumed that the mutant reacts similarly to the antibodies as the wild type. Oocyte membranes were patched in the cell-attached configuration, and single-channel events were recorded in the presence of 4 $\mu$M ACh (in order to avoid channel block or desensitization by the high agonist concentration) and 10 $\mu$g/$\mu$L mAb or Fab.

Table 2: Results of Single-Channel Analysis[a]

| sample | short open time (ms) | long open time (ms) | amplitude (pA) | results |
|---|---|---|---|---|
| control | 0.82 ± 0.04 | 11.6 ± 2.02 | 10.4 ± 0.4 | − |
| mAb 35 | 0.77 ± 0.03 | 3.97 ± 1.76 | 10.2 ± 0.6 | no effect |
| mAb 132 | 1.04 ± 0.04 | undefined | 10.1 ± 0.4 | no effect |
| mAb 247 | − | − | − | blocks activity |
| Fab 247 | − | − | − | blocks activity |
| mAb 370 | 0.79 ± 0.05 | undefined | 9.3 ± 0.4 | no effect |
| mAb 371 | 0.54 ± 0.06 | 9.62 ± 3.08 | 10.0 ± 0.8 | no effect |
| mAb 383 | − | − | − | blocks activity |
| mAb 387 | 0.62 ± 0.04 | 12.1 ± 8.6 | 8.2 ± 0.2 | reduces condactance |
| Fab 387 | − | − | − | blocks activity |

[a] *X. laevis* oocytes expressing *Torpedo* wild type or αG421W nAChR were patched with a micropipette containing 4 $\mu$M ACh and 10 mg/mL mAb or Fab. The holding potential was set at −100 mV, and the temperature was held at 18 °C.

The results of the patch clamp experiments are summarized in Table 2. In the absence of mAb, the αG421W control had two open times of 0.82 ± 0.04 and 11.6 ± 2.0 ms, respectively (Figure 1A,B). In the presence of mAb 35, mAb 132, and mAb 370, the short open times of the nAChR−mAb complexes were similar to that of the control. The short and long open time constants for mAb 35 were 0.77 ± 0.03 and 3.97 ± 1.76 ms, respectively (Figure 2). mAb 132 and mAb 370 had short open times of 1.04 ± 0.04 and 0.79 ± 0.05 ms, respectively (Figures 3 and 4). Although the much longer second open times vary, the open time histograms of these mAb−nAChR complexes are similar to that of the control. Therefore, we conclude that these antibodies do not affect channel gating. The single-channel amplitudes for each mAb−nAChR complex are listed in Table 2.

A marked decrease in the frequency of channel openings over time was observed after patching in the presence of mAb 247 and mAb 383. Pre- and post-control patches without addition of mAb in the patch pipet on the same oocyte did not exhibit this decline. It is presumed that mAb 247 is binding to the nAChR and blocking subsequent channel activity by either preventing channel opening or physically occluding the channel pore. The data are presented on a frequency histogram (Figure 6). The Fab fragment of mAb 247 behaved in a manner similar to that of the mAb 247 by arresting channel opening (data not shown). mAb 387 did not affect single-channel open time but slightly reduced the single-channel amplitude approximately 20% (Figure 7), while Fab 387 blocked channel activity completely (data not shown).

*[$^{125}$I]TID Labeling of Antibody−nAChR Complexes.* In order to investigate how antibody binding to the nAChR affects the structural transitions of nAChR, we used [$^{125}$I]-

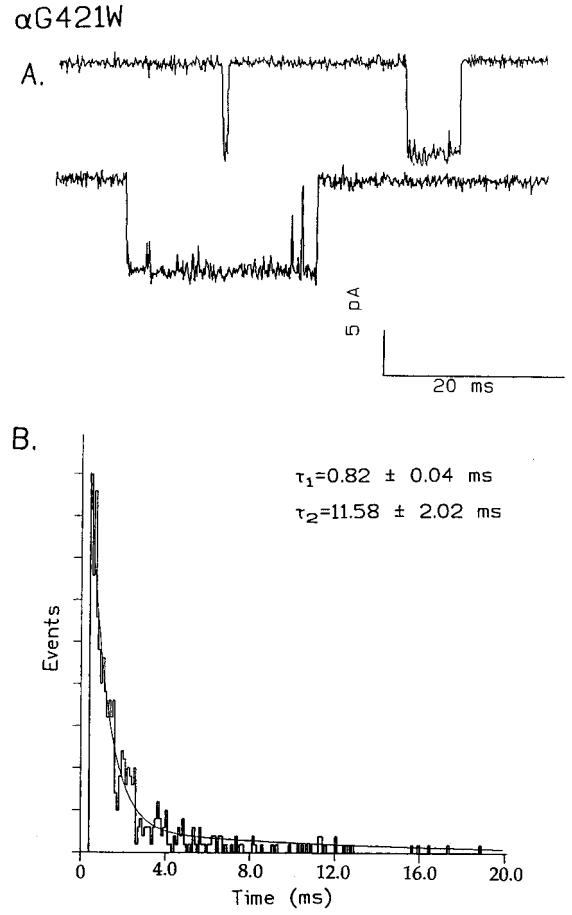


FIGURE 1: (A) Single-channel traces of αG421W receptor in the absence of antibody. (B) Open time histogram of 1013 events fit with two exponentials corresponding to open times of 0.82 ± 0.04 and 11.6 ± 2.02 ms.

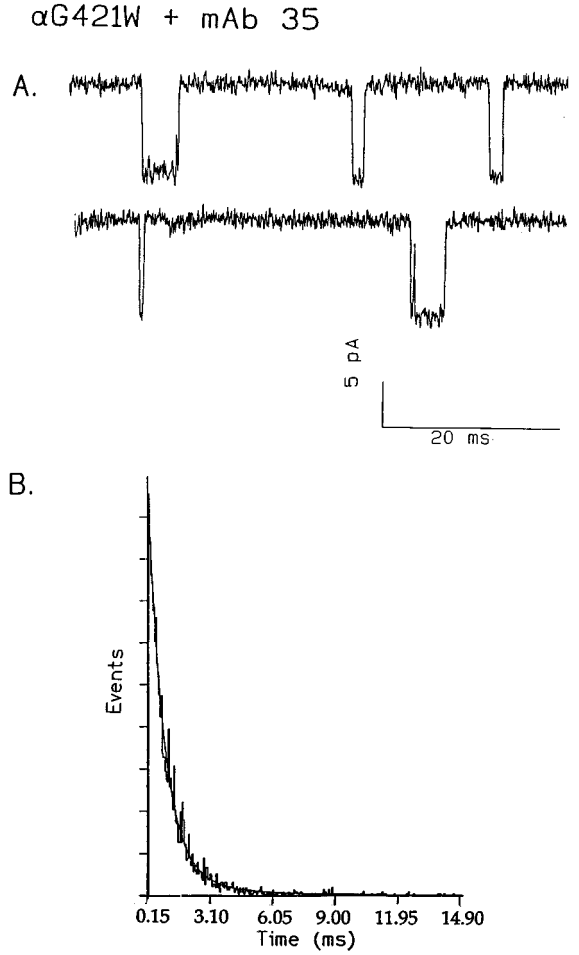


FIGURE 2: (A) Single-channel traces of αG421W receptor in the presence of mAb 35. (B) Open time histogram of 3476 events fit with two exponentials corresponding to open times of 0.77 ± 0.03 and 3.97 ± 1.76 ms.

TID labeling of nAChR subunits. nAChR was purified from *T. californica* electroplax tissue by affinity chromatography and reconstituted into membranes composed of phosphatidylcholine (PC), phosphatidic acid (PA), and cholesterol (CH). The nAChR was then incubated with several monoclonal antibodies and subsequently exposed to high concentrations of carbamylcholine (carb) which induces a desensitized state (+carb). After addition of [$^{125}$I]TID and ultraviolet exposure, the nAChR subunits were separated by SDS−PAGE. The bands on the gel were visualized by autoradiography and phosphorimaging. The relative intensities of the $\gamma$-subunit bands were measured because this band is most sensitive to the presence of agonist under the conditions used. The addition of carb decreased labeling of the nAChR $\gamma$-subunit by 30−70% compared to those of samples without carb (−carb). The [$^{125}$I]TID labeling pattern was also examined for nAChR preincubated with carb prior to the addition of antibody (p+carb). In the absence of nAChR, none of the mAbs reacted with [$^{125}$I]TID.

In the presence of mAb 247 (Figure 8), there was a 59% (+carb) and a 57% (p+carb) decrease in labeling of $\gamma$-subunit with respect to the +mAb/−carb sample. The control (without addition of mAb) showed a 39% decrease between the +carb and −carb. This result indicated that mAb 247, which was shown to block the opening of the channel by patch clamp experiments, still allowed nAChR to undergo the transition between the resting and carb-induced desensitized state.

The experiments in the presence of mAb 370 also suggested that the nAChR underwent the normal resting to desensitized transition. There was a 31% decrease in labeling for the +carb sample compared to the −carb sample (Figure 9). On this gel, the control in the absence of antibody (−mAb) showed a 50% decrease. The p+carb sample showed a 38% decrease compared to −carb. Interestingly, mAb 370 enhanced the labeling of both the resting and carb-induced desensitized states compared to the −mAb controls. There was a 2.2-fold increase in the level of $\gamma$-subunit radiolabeling of the resting state as compared to that of the −mAb/−carb control and a 2.7-fold increase for the +carb as compared to the −mAb/+carb sample. The pre-desensitized receptor also showed a 2.4-fold increase in the $\gamma$-subunit labeling as compared to the −mAb/+carb control.

The labeling studies also demonstrated that mAb 387 did not prevent the transition from the resting to the carb-induced desensitized state. In the gel shown in Figure 10, there was a 64 and 65% decrease for the +mAb/+carb and +mAb/p+carb samples, respectively, compared to +mAb/−carb. The −mAb/+carb control had a 27% decrease with respect to −mAb/−carb on the gel shown. Interestingly, mAb 387 also enhances the labeling of the $\gamma$-subunit, but only in the resting state. It was calculated that this increase was 1.8-fold.

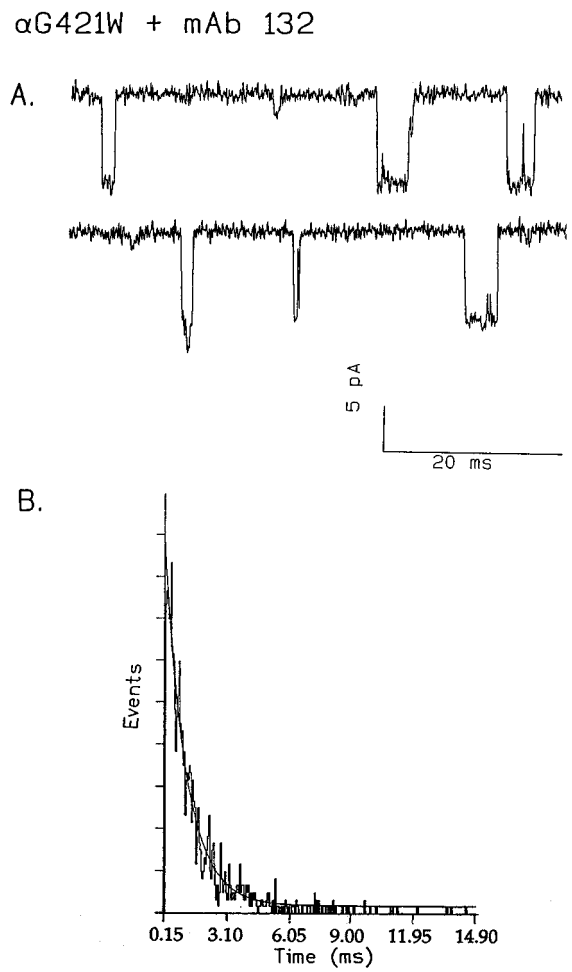


FIGURE 3: (A) Single-channel traces of αG421W receptor in the presence of mAb 132. (B) Open time histogram of 1190 events fit with two exponentials. The first open time was 1.04 ± 0.04 ms, but the second open time was not able to be fit accurately.

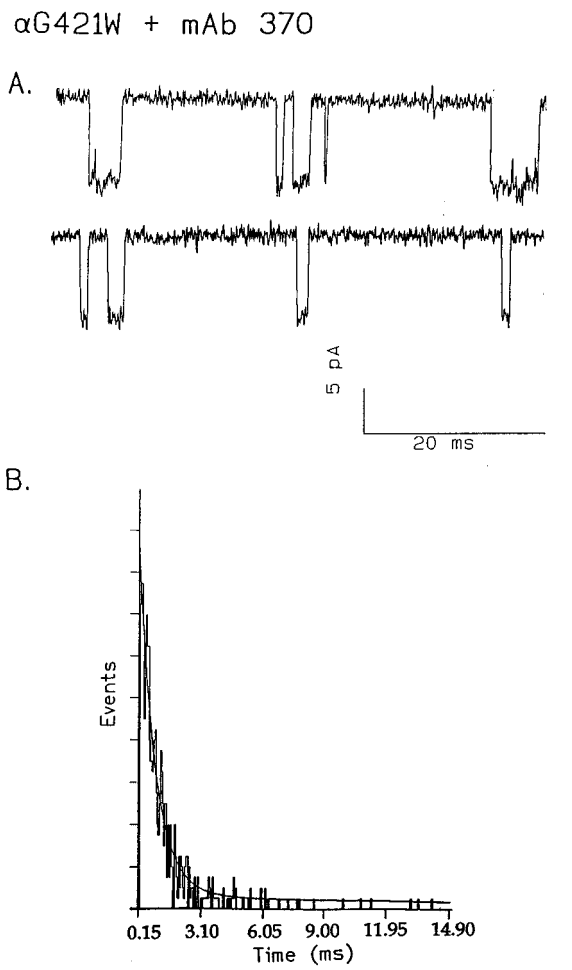


FIGURE 4: (A) Single-channel traces of αG421W receptor in the presence of mAb 370. (B) Open time histogram of 589 events fit with two exponentials. The first open time was 0.79 ± 0.05 ms. The second open time could not be fit.

## DISCUSSION

In this study, we used single-channel analysis and photoaffinity labeling to gain new insights into nAChR structure and function. Our results, in conjunction with the information from earlier experiments, support the idea of the allosteric linkages between the antibody epitope and ligand binding sites proposed by Maelicke (1987).

The patch clamp analysis revealed that mAb 35 and mAb 132 do not have significant effects on nAChR open time or conductance. mAb 35 and mAb 132 recognize the main immunogenic region (MIR) of the nAChR (Tzartos & Lindstorm, 1980; Agius et al., 1988). This region, located at α67−76, is the target of most anti-nAChR antibodies (Tzartos & Lindstorm, 1980; Papadouli et al., 1993). However, these mAbs do not affect carb, α-BTX, or *d*-tubocurare (d-Tc) binding to the nAChR as summarized in Table 1. It is likely that mAb 35 and mAb 132 do not affect nAChR activity because the MIR does not lie near functionally sensitive regions nor is it allosterically linked to the cholinergic site or gating regions. It may be argued that antibodies may be binding to and blocking only a fraction of the channels in the patch. The receptors that are not complexed with mAb will open with normal gating parameters to give the illusion that the mAb does not affect activity. In this study, however, the concentration of antibody within the pipette is very high compared to the small number of receptors in the patch. In addition, the binding of mAb to nAChR was tested by ELISA. Fast and complete binding is observed with mAb 247 and mAb 383 which were able to block channel activity in seconds to minutes. Therefore, it is assumed that all of the receptors in the patch are associated with the mAb and the openings are from mAb−nAChR complexes.

It has been demonstrated that mAb 247 can differentiate between the two α-BTX sites on the nAChR by blocking only the kinetically resolved slow component of toxin binding without altering carb binding, and the stoichiometry of binding of mAb 247 to nAChR is 1:1 (Mihovilovic et al., 1984). The toxin competition assay also indicates that the mAb epitope and the α-BTX binding site are separate, allosterically linked regions. Another property of mAb 247 is that it can shift the high-affinity d-Tc site to a low-affinity site without changing the stoichiometry of binding; however, d-Tc does not block mAb binding (Mihovilovic et al., 1987). The high-affinity d-Tc site has been identified at the α-subunits−γ-subunit interface, while the low-affinity site has been localized at the α-subunit−δ-subunit interface (Blount & Merlie, 1989; Sine & Claudio, 1991). These results suggest that the epitope is not in the acetylcholine binding site, but allosteric mechanisms are affecting d-Tc affinity (Mihovilovic et al., 1984). Since the mAb 247 is blocking only a single α-BTX site and the high-affinity d-Tc site, we can assume that the antibody has specificity for only

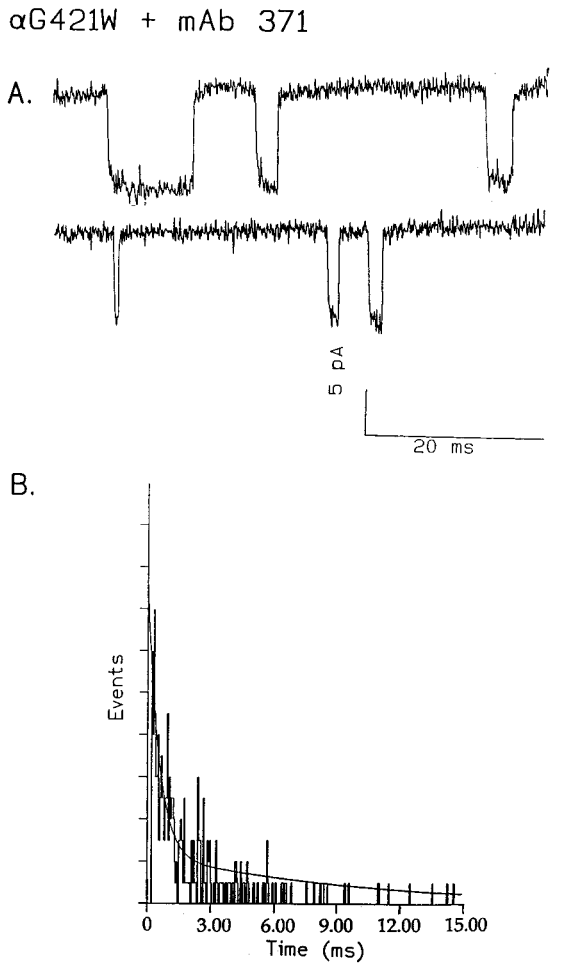


FIGURE 5: (A) Single-channel traces of αG421W receptor in the presence of mAb 371. (B) Open time histogram of 261 events fit with two exponentials corresponding to open times of 0.54 ± 0.03 and 9.62 ± 3.08 ms.

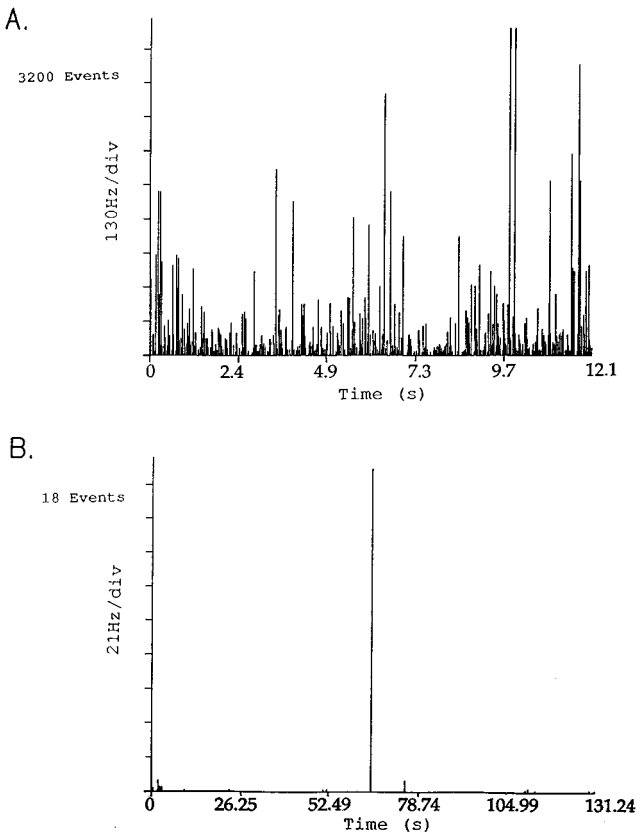


FIGURE 6: (A) Instantaneous frequency plot of control wild type nAChR openings in a single-channel patch. Approximately 3200 openings occurred within 12 s. (B) Upon application of 10 mg/mL mAb 247, the frequency of opening is dramatically reduced. Only 18 openings were detected in 131 s.

one of the α-subunits which is likely to be adjacent to the γ-subunit.

The patch clamp data presented here demonstrate that mAb 247 blocks ion channel activity. The loss of channel activity could be caused by the mAb either directly preventing nAChR opening or physically occluding the ion channel. If mAb 247 bound to the α-subunit−γ-subunit interface blocks the ion channel physically, we would be able to detect the flow of ions by reducing the size of obstruction. However, the Fab fragment of mAb 247, which has only $^1/_3$ of the mass of the mAb (50 kDa), also blocked nAChR activity completely. Therefore, we concluded that mAb 247 is able to arrest conformation changes that are responsible for the opening of the nAChR channel. This antibody can serve as a valuable tool because it is able to decouple agonist binding from channel opening.

Although mAb 247 blocks channel opening, the photolabeling experiments determined that antibody binding does not impede the resting to desensitized transition. These results support an earlier study which demonstrated using an α-BTX competition assay that the mAb 247−nAChR complex could desensitize (Mihovilovic et al., 1987). Taken with the patch clamp results, this result demonstrates that the nAChR can shift from a resting state to a desensitized state without prior channel opening. This supports kinetic models which postulate that the liganded closed state can transition to a desensitized state (Cash & Hess, 1980; Ochoa et al., 1989), although these data do not preclude desensitization proceeding from the open state. How this antibody alters nAChR function is not known, but it is possible to speculate that the antibody is probably binding to an epitope on the α-subunit and interfering with the agonist-induced conformational changes within the α-subunit that trigger channel gating. Alternatively, mAb 247 may have an epitope that is comprised of determinants from two subunits, and its binding prevents movement of the subunits relative to each other. The sliding of subunits against each other has been proposed as a mechanism of channel opening (Unwin & Zampighi, 1980; Galzi et al., 1991).

mAb 370 did not alter single-channel behavior during this study. This was unexpected because previous studies imply that the antibody has immediate and severe effects on ion channel function. The epitope of mAb 370 has been mapped to 187−205 in each α-subunit which includes residues involved in ACh, nicotine, and α-BTX binding (Chinchetru et al., 1989). In addition, this antibody has been shown to cause a hyperacute form of experimental autoimmune myasthenia gravis paralysis in chicken hatchlings soon after injection (Gomez & Richman, 1983) and irreversibly reduce the miniature end-plate potentials and end-plate currents in chicken muscle (Maselli et al., 1989). The reason for the discrepancy between our electrophysiological data and previous studies is not apparent. Although high concentrations of carb inhibit the binding of mAb 370, the low concentrations used in patch clamping should not prohibit mAb binding (Mihovilovic et al., 1987; Chinchetru et al., 1989). It is likely that mAb 370 is binding to the nAChR, but not

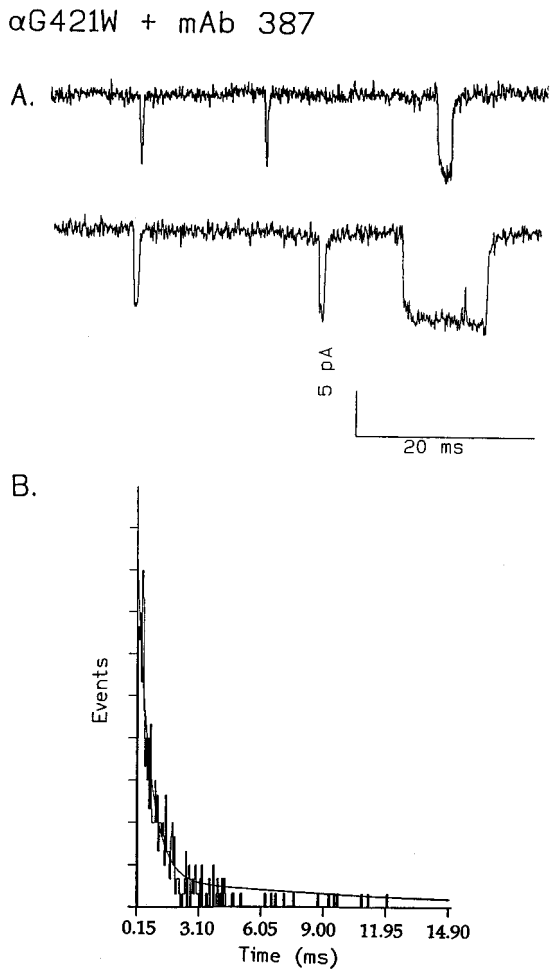


FIGURE 7: (A) Single-channel traces of αG421W receptor in the presence of mAb 387. (B) Open time histogram of 261 events fit with two exponentials corresponding to open times of 0.54 ± 0.03 and 9.62 ± 3.08 ms.

influencing channel gating. The whole cell patch clamp or outside-out patch which can examine a population of channels may provide better information about mAb 370-nAChR interactions.

The photolabeling studies established that the mAb 370−nAChR complex can proceed to a desensitized state. This supports the patch clamp data that show that nAChR can be activated in the presence of mAb 370. Interestingly, the level of $\gamma$-subunit labeling of both the resting and desensitized states is enhanced considerably. Additionally, the image shows that the labeling of the α- and $\beta$-subunits is also increased. The enhancement of labeling could reflect changes in either the stoichiometry or the equilibrium of [$^{125}$I]-TID binding. If we assume that it changes the stoichiometry, the 2−3-fold increase implies the formation of at least one new site. This new site would likely have to be in the pore to be able to increase the labeling of multiple subunits. It is more likely, however, that the binding equilibrium at the high-affinity channel site is being altered. The mAb binding may change the conformation of the ion channel in a way that would increase photolabel association in both the resting and desensitized states. This supports the current model that the cholinergic site, which includes the mAb 370 epitope, is allosterically linked to the pore to effect channel gating.

mAb 387 was also shown to alter the function of the nAChR. It has been determined that one molecule of mAb 387 inhibits the association of carb at the two agonist binding

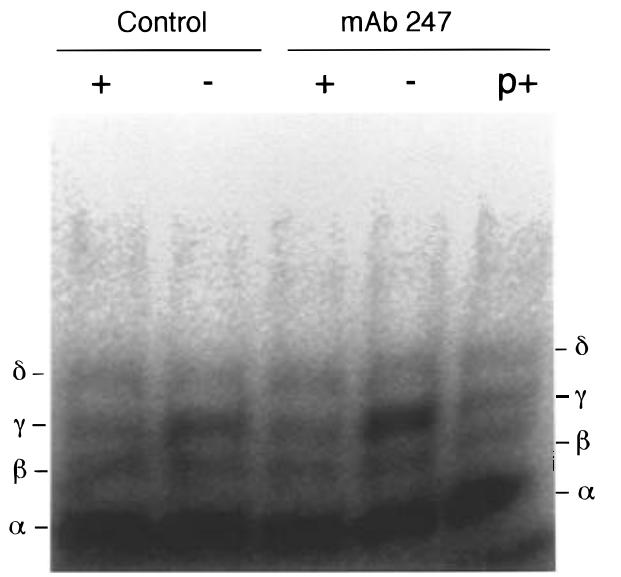


FIGURE 8: Phosphorimage of an SDS−PAGE gel containing [$^{125}$I]-TID-labeled nAChR subunits. nAChR was incubated with mAb 247 for 30 min. The control samples were not exposed to antibody. + and − represent the presence and absence of 1 mM carb, respectively, prior to the addition of the photolabel. p+ represents a 5 min carb preincubation of the nAChR before the addition of mAb 247.

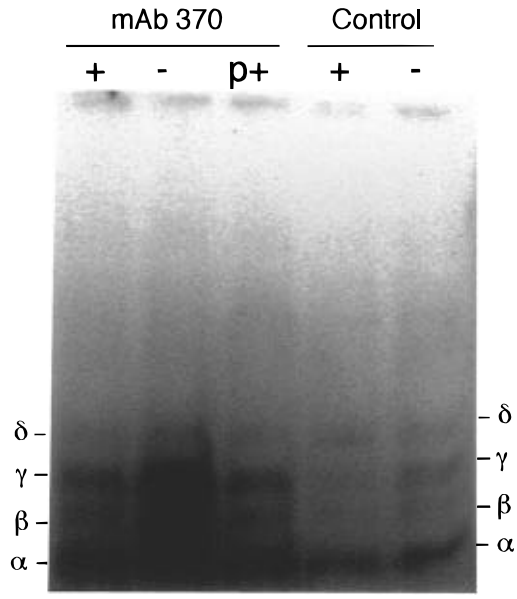


FIGURE 9: Phosphorimage of an SDS−PAGE gel containing [$^{125}$I]-TID-labeled nAChR subunits. nAChR was incubated with mAb 370 for 30 min, and the control samples were not exposed to antibody. + and − represent the presence and absence of 1 mM carb, respectively, prior to the addition of the photolabel. p+ represents a 5 min carb preincubation of the nAChR before the addition of mAb 370.

sites, suggesting that mAb 387 can cross-link the α-subunits of a single molecule of nAChR (Mihovilovic et al., 1987). Although it can completely inhibit carb binding and eliminates the high-affinity d-Tc site, it only blocks 25% of the α-BTX sites (Mihovilovic et al., 1987). Furthermore, carb and d-TC do not prevent mAb binding, but α-BTX does (Mihovilovic et al., 1987). These complicated interactions suggest that the mAb 387 epitope is part of an elaborate allosteric network.

Since mAb 387 was found to block the association of agonist with the nAChR, we were surprised to see single-

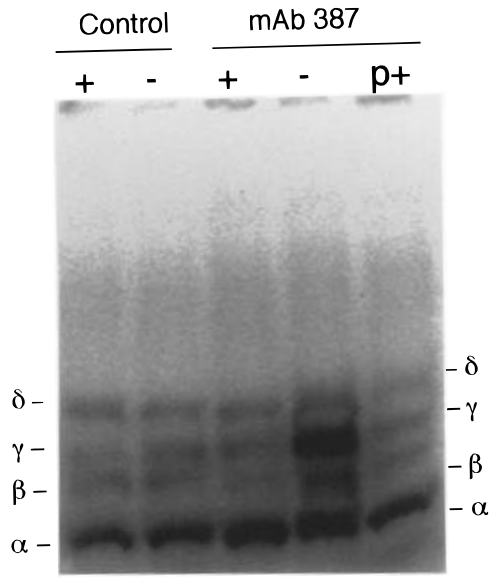


FIGURE 10: Phosphorimage of an SDS−PAGE gel containing [$^{125}$I]-TID-labeled nAChR subunits. nAChR was incubated with mAb 387 for 30 min, and the control samples were not exposed to antibody. + and − represent the presence and absence of 1 mM carb, respectively, prior to the addition of the photolabel. p+ represents a 5 min carb preincubation of the nAChR before the addition of mAb 387.

channel openings. The mean channel open time of the mAb 387−nAChR complexes was similar to that of the control, but the amplitude was reduced at least 20%. A decline in amplitude could be caused by structural alterations within the pore which could have either changed the chemical environment or narrowed the diameter of the channel. Alternatively, the opening at the top of the channel could be partially occluded by the mAb. The labeling experiments demonstrate that the nAChR−mAb 387 complex can be desensitized. The level of $\gamma$-subunit labeling of the resting state is increased approximately 2-fold, but the desensitized state has normal labeling. Other subunits such as the $\beta$- and $\delta$-subunits have increased labeling in the resting state also. Again, this implies that the antibody is changing the binding equilibrium at the [$^{125}$I]TID high-affinity site in the pore. Since the change in labeling reflects mAb-induced changes in the structure of the pore, this may be responsible for the decrease in the amplitude rather than steric obstruction. The Fab fragment was generated to differentiate between these two possibilities. It was expected that, if the mAb was reducing amplitude by steric occlusion, the smaller Fab would decrease the ion flow much less. Patch clamp experiments with the Fab showed that it did not have either of the expected outcomes, but it completely blocked channel activity. This means that interactions of this antibody with the nAChR may be much more complex than the two models presented. More experiments must be carried out to find out how the mAb is lowering single-channel conductance.

Our data, in combination with earlier studies, show that mAbs have diverse modes of action on the receptor. mAbs that bind to the MIR (mAb 35 and 132) do not have effects on the single-channel conductance or open time. One antibody (mAb 383) inhibits agonist association to the receptor and, therefore, prevents channel activation. Another antibody (mAb 247) which allows the binding of agonist prevents the receptor from transitioning to an open state. This antibody may in the future be used as a tool to separate agonist activation from channel opening. We also discovered an antibody that does not have "all-or-none" consequences on nAChR function. mAb 387 decreases the single-channel amplitude. It is speculated that either mAb cross-linking partially occludes the top of the channel or the mAb is altering the structure of the pore itself. Additionally, photolabeling studies demonstrate that the nAChR can undergo the resting to desensitized transitions while bound to antibodies. These experiments also suggest that some antibodies can cause structural alterations in the channel pore.

## ACKNOWLEDGMENT

We thank Dr. Richard Nuccitelli for use of the facilities for oocyte injection and Dr. David Richman and Dr. Robert Fairclough for providing us supernatants for mAbs. We also thank Barbara Birks, Gregor Zimmerman and Judy Butler for RNA preparation and oocyte injection.

## REFERENCES

Agius, M. A., Geannopoulos, C. J., Fairclough, R. H., & Richman, D. P. (1988) *J. Immunol. 140*, 62−68.
Beck, W., Jung, G., Bessler, W. G., Benz, I., & Kohlhardt, M. (1994) *Biochim. Biophys. Acta 1206*, 263−271.
Betz, H. (1990) *Neuron 5*, 383−392.
Blanton, M. P., & Cohen, J. B. (1992) *Biochemistry 31*, 3738−3750.
Blanton, M. P., & Cohen, J. B. (1994) *Biochemistry 33*, 2859−2872.
Blount, P., & Merlie, J. P. (1989) *Neuron 3*, 349−357.
Cash, D. J., & Hess, G. P. (1980) *Proc. Natl. Acad. Sci. U.S.A. 77*, 842−846.
Chinchetru, M. A., Marquez, J., Garcia-Borron, J., Richman, D. P., & Martinez-Carrion, M. (1989) *Biochemistry 28*, 4222−4229.
Conti-Tronconi, B. M., McLane, K. E., Raftery, M. A., Grando, S. A., & Protti, M. P. (1994) *Crit. Rev. Biochem. Mol. Biol. 29*, 69−123.
DiPaola, M., Czajkowski, C., & Karlin, A. (1989) *J. Biol. Chem. 264*, 15457−15463.
Donnelly, D., Mihovilovic, M., Gonzalez-Ros, J. M., Ferragut, J. A., Richman, D. P., & Martinez-Carrion, M. (1984) *Proc. Natl. Acad. Sci. U.S.A. 81*, 7999−8003.
Dowding, A. J., & Hall, Z. W. (1987) *Biochemistry 26*, 6372−6381.
Fairclough, R. H., Josephs, R., & Richman, D. P. (1993) *Ann. N. Y. Acad. Sci. 681*, 113−125.
Galzi, J.-L., Revah, F., Bessis, A., & Changeux, J.-P. (1991) *Ann. Rev. Pharmacol. 31*, 37−72.
Gomez, C. M., & Richman, D. P. (1983) *Proc. Natl. Acad. Sci. U.S.A. 80*, 4089−4093.
Gomez, C. M., & Richman, D. P. (1985) *J. Immunol. 135*, 234−241.
Karlin, A. (1993) *Curr. Opin. Neurobiol. 3*, 299−309.
Lasalde, J. A., Ortiz-Miranda, S., Butler, D. H., Tamamizu, S., Vibat, C. R. T., Pappone, P., & McNamee, M. G. (1995) *Biophys. J. 68* (2), A233.
Li, L., Schuchard, M., Palma, A., Pradier, L., & McNamee, M. G. (1990) *Biochemistry 29*, 5428−5436.
Lowry, O. H., Rosebrough, N. J., Farr, A. L., & Randall, R. J. (1951) *J. Biol. Chem. 193*, 265−275.
Maelicke, A. (1987) *Biochem. Soc. Trans. 15*, 108−112.
Maselli, R. A., Nelson, D. J., & Richman, D. P. (1989) *J. Physiol. 411*, 271−283.
McCarthy, M. P., & Stroud, R. M. (1989) *J. Biol. Chem. 264*, 10911−10916.
McClare, C. W. F. (1971) *Anal. Biochem. 39*, 527−530.
McNamee, M. G., Jones, O. T., & Fong, T. M. (1986) in *Ion Channel Reconstitution* (Miller, C., Ed.) pp 231−273, Plenum, New York.
Mihovilovic, M., & Richman, D. P. (1984) *J. Biol. Chem. 259*, 15051−15059.

Mihovilovic, M., & Richman, D. P. (1987) *J. Biol. Chem. 262*, 4978−4986.
Mishina, M., Kurosaki, T., Tobimatsu, T., Morimoto, Y., Noda, M., Yamamoto, T., Terao, M., Lindstorm, J., Takahashi, T., Kuno, M., & Numa, S. (1984) *Nature 307*, 604−608.
Noda, M., Takahashi, H., Tanabe, T., Toyosato, M., Kikyotani, S., Furutani, Y., Hirose, T., Takashima, H., Inayama, S., Miyata, T., & Numa, S. (1983) *Nature 302*, 528−532.
Ochoa, E. L. M., Dalziel, A. W., & McNamee, M. G. (1983) *Biochim. Biophys. Acta 727*, 151−162.
Ochoa, E. L., Chattopadhyay, A., & McNamee, M. G. (1989) *Cell. Mol. Neurobiol. 9*, 141−78.
Papadouli, I., Sakarellos, C., & Tzartos, S. J. (1993) *Eur. J. Biochem. 211*, 227−234.
Pradier, L., & McNamee, M. G. (1992) *in The Structure of Biological Membranes* (Yeagle, P., Ed.) pp 1047−1106, Telford, Caldwell, NJ.
Sachs, F., Neil, J., & Barkakati, N. (1982) *Pfluegers Arch. 395*, 331−340.
Sine, S. M., & Claudio, T. (1991) *J. Biol. Chem. 266*, 19369−19377.
Tzartos, S. J., & Lindstorm, J. M. (1980) *Proc. Natl. Acad. Sci. U.S.A. 77*, 755−759.
Unwin, N. (1993) *Cell 72* (Suppl.), 31−41.
Unwin, P. N. T., & Zampighi, G. (1980) *Nature 283*, 545−549.
Valenzuela, C. F., Dowding, A. J., Arias, H. R., & Johnson, D. A. (1994) *Biochemistry 33*, 6586−6594.
Watters, D., & Maelicke, A. (1983) *Biochemistry 22*, 1811−1819.
White, B. H., & Cohen, J. B. (1992). *J. Biol. Chem. 267*, 15770−15783.
White, B. H., Howard, S., Cohen, S. G., & Cohen, J. B. (1991) *J. Biol. Chem. 266*, 21595−21607.
Xu, Q., Fairclough, R. H., & Richman, D. P. (1993a) *Ann. N. Y. Acad. Sci. 681*, 172−174.
Xu, Q., Twaddle, G. M., Richman, D. P., & Fairclough, R. H. (1993b) *Ann. N. Y. Acad. Sci. 681*, 175−178.

BI960369U